Award Number: **W81XWH-10-1-0950**

TITLE: Development and Translation of a Tissue-Engineered Disc in a Preclinical Rodent Model

PRINCIPAL INVESTIGATOR: Robert L Mauck, PhD

CONTRACTING ORGANIZATION: Philadelphia Research and Education Foundation
Philadelphia, PA 19104

REPORT DATE: February 2014

TYPE OF REPORT: Final Report

PREPARED FOR: U.S. Army Medical Research and Materiel Command
Fort Detrick, Maryland 21702-5012

DISTRIBUTION STATEMENT:

X Approved for public release; distribution unlimited

REPORT DOCUMENTATION PAGE

Form Approved
OMB No. 0704-0188

1. REPORT DATE *(DD-MM-YYYY)*	2. REPORT TYPE	3. DATES COVERED
February 2014	FINAL REPORT	30Sep2010 - 29Sep2013

4. TITLE AND SUBTITLE

Development and Translation of a Tissue-Engineered Disc in a Preclinical Rodent Model

5a. CONTRACT NUMBER
W81XWH-10-1-0950

5b. GRANT NUMBER

5c. PROGRAM ELEMENT NUMBER

6. AUTHOR(S)
Robert L Mauck, PhD
Nader M. Hebela, MD
Dawn M. Elliott, PhD
email: lemauck@mail.med.upenn.edu

5d. PROJECT NUMBER

5e. TASK NUMBER

5f. WORK UNIT NUMBER

7. PERFORMING ORGANIZATION NAME(S) AND ADDRESS(ES)

Philadelphia Research and Education Foundation
Philadelphia, PA 19104

8. PERFORMING ORGANIZATION REPORT NUMBER

9. SPONSORING / MONITORING AGENCY NAME(S) AND ADDRESS(ES)
U.S Army Medical Research and Materiel Command
Fort Detrick, Maryland 21702-5012

10. SPONSOR/MONITOR'S ACRONYM(S)

11. SPONSOR/MONITOR'S REPORT NUMBER(S)

12. DISTRIBUTION / AVAILABILITY STATEMENT

Approved for public release; distribution unlimited

13. SUPPLEMENTARY NOTES

14. ABSTRACT

Disc injury through trauma, vibration loading, or mechanical overload, and the resulting disc degeneration in response to these insults over time are tremendous problems affecting the active and veteran military population. Current treatment options fail to restore disc structure and mechanical function. Our goal in this proposal is to develop methodologies for the engineering and implanting of a functional biologic disc replacement. Significant progress has been made in the last 12 months towards achieving this goal. We have successfully engineered a concentric annulus fibrosus, the functional properties of which improve with culture time. We have shown the dynamic culture further enhances functional matrix deposition. We have shown that a short period of exposure to transforming at a high dose is equal to or better than long term exposure for stem cells cultured in an engineered nucleus pulposus-like hyaluronan hydrogel. We have developed and validated a minimally invasive surgical technique for implantation of our engineered disc. We have successfully performed in implantation of acellular engineered discs. Finally, we have designed and implemented a novel internal fixation device to enhance retention of the engineered disc and stabilize the joint during healing.

15. SUBJECT TERMS
Intervertebral disc degeneration; low back pain; biological disc replacement; preclinical animal model

16. SECURITY CLASSIFICATION OF:			17. LIMITATION OF ABSTRACT	18. NUMBER OF PAGES	19a. NAME OF RESPONSIBLE PERSON
a. REPORT	b. ABSTRACT	c. THIS PAGE			USAMRMC
U	U	U	UU	27	19b. TELEPHONE NUMBER *(include area code)*

Table of Contents

	Page
Introduction……..…….…..	**2**
Body……..	**2**
Key Research Accomplishments…….……..	**22**
Reportable Outcomes……	**22**
Conclusions……	**23**
References/Publications…..……	**23**
Appendices……	**25**

Introduction:

The focus of this project was on the restoration of the intervertebral disc through tissue engineering methodologies. Disc injury through trauma, vibration loading, or mechanical overload, and the resulting disc degeneration in response to these insults over time are tremendous problems affecting the active and veteran military population. Neither conservative treatments, such as stretching and exercise, nor surgical options, such as fusion and arthroplasty, restore disc structure or mechanical function. Total disc arthroplasty is relatively new to clinical practice, but suffers from the same problems as traditional implant materials – wear and the need for eventual replacement. An alternative to these methods involves implantation with a biologic tissue engineered replacement. Such a biologic tissue restoration method would not be subject to wear as occurs with prosthetic devices, and would restore flexibility and motion about that spinal segment. Because the function of the disc is mechanical, it is important to focus upon mechanics in the design of functional tissue engineered constructs (TECs) and to direct the biology (maintenance of phenotype and ECM deposition) towards these mechanical outcomes. Direct biologic restoration of the disc with a TEC that duplicates the mechanical properties of the native tissue and restores range of motion would be an ideal alternative. Our goal in this project was to develop methodologies for the engineering and implanting of a functional biologic disc replacement. **The objective of this proposal was to move to the translational space and towards clinical implementation by creating and implanting a tissue engineered disc-like angle ply structure (DAPS)**, and throughout this development, to remain mindful of the fundamental importance of the mechanical function.

During the three years of funding on this project (which was extended to four years through a no cost extension), the PIs made substantial progress in the Aims. Given the highly collaborative and interdisciplinary activities of this project, a single document detailing all progress is presented. The research team has met on a weekly or bi-weekly basis over this time course, and have established major advances in the formation of disc-like angle-ply structures for disc tissue engineering applications, as will be detailed below.

Body:

Drs. Elliott, Mauck, and Hebela have successfully completed all aims in their project (OR090090) entitled: “Development and Translation of a Tissue-Engineered Disc in a Preclinical Rodent Model”. Below, we provide a listing of the original three aims of our project, followed by detailed descriptions of work completed within these Aims. Our work stems from the translation of the single and bi-layer constructs with tensile properties approaching that of the native annulus fibrosus tissue into full 3D Disc-like Angle Ply Structures (DAPS), inclusive of a hyaluronic acid hydrogel seeded with adult stem cells, that can be used to replace the degenerate native disc.

<u>Aim 1</u>: Create a mesenchymal stem cell (MSC) seeded 3D structural TEC disc from concentric AF constructs surrounding an engineered nucleus pulposus (NP) composed of a hyaluronic acid (HA) hydrogel. Measure the disc structural mechanics in compression and torsion, and the isolated AF and NP substructures in compression following time in culture. Evaluate the molecular, histological, and biochemical

properties of these TEC discs as a function of time in culture and with variations in media conditions.

Aim 1 has been in completed full. In a series of studies, we worked on developing the AF portion of the DAPS, followed by a study focused on the NP portion of the DAPS (the NP-seeded HA hydrogel), followed by culture of a full AF+NP DAPS construct.

Optimization of the Tissue Engineered AF Region:
In our first study, we investigated the biochemical and mechanical effects of orbital shaking on the maturation of multi-lamellar disc-like angle-ply structures (DAPS) in order to expedite growth conditions for AF replicates and, more broadly, to optimize design strategies for MSC-laden multi-layered tissues. This work was published in abstract form as: **Functional Enhancement of Disc-Like Angle-Ply Structures via Dynamic Culture**, by Kluge, JA; Martin, JT; Nerurkar, NL; Amaniera, FA; Pampati, RA; Elliott, DM; Mauck R L, at the 2011 Othopaedic Research Society in Long Beach, California. A full length manuscript on this work is now under construction and is expected to be submitted soon.

Briefly, the focus and findings of this work were as follows. We formed an annulus fibrosus (AF scaffold) by electrospinning aligned PCL fiber mats ~0.3mm thick. 3 mm wide strips were cut 30^o from the fiber direction. Strips were seeded with MSCs and pre-cultured for 2 weeks in chemically defined media with 10 ng/mL TGF-β3. Media was changed twice weekly for the duration of the study. At 0 weeks, strips were paired into bilayers with opposing +/-30^o fiber orientations and wrapped concentrically to 10mm outer diameter. After 1 week, the cup holding the DAPS construct was removed to allow for free swelling culture with all surfaces exposed. At this baseline (week 0) or 4 weeks after removing from the retaining cups, DAPS were harvested for analysis. Alternatively, after removing from retaining cups, DAPS were maintained on an orbital shaker set to a 2Hz frequency and likewise harvested at 4 weeks. This was done to improve maturation and to simulate fluid exchange that might be expected in vivo with mechanical loading. Samples were reserved for torsion testing (n=3), in which a custom-designed rig, containing a torque cell (5in.-oz. limit) in series with a stepper motor (LabVIEW controlled), was affixed to a standard Model 5542 Instron uniaxial testing device. Samples were compressed to a creep load of 0.02N for 200 seconds, followed immediately by 25% axial compression of the post-creep height. After a 20 minute relaxation period, DAPS were subjected to 10 cycles of torsion at +/- 6° at 0.05Hz and the last load/unload curve reserved for analysis. Raw torque data was normalized to construct geometry to calculate torsional stiffness [kPa] and range of torque [kPa/°]. Following testing, DAPS samples were stored frozen, lyophilized, papain digested and assayed for collagen, GAG, and DNA content. Likewise, media in both shaken and static cultures were periodically reserved during feeding and measured for GAG content using the DMMB assay. Untested samples (n=2) were sectioned and stained with DAPI, Alcian Blue, and Picrosirius Red to visualize cells, proteoglycans, and collagen, respectively. Significance was determined by one-way ANOVA with Tukey's post hoc ($p \leq 0.05$).

In carrying out this work, we found that both statically and dynamically cultured MSC-laden DAPS increased in torsional mechanical properties and biochemical content with time in culture. By 4 weeks, PG staining (Alcian Blue, **Fig. 1**), was significantly improved in both static and dynamic groups, but was more homogenous throughout constructs with dynamic culture. Although there was a significant increase in total GAG in dynamic culture groups compared to their static counterparts (**Fig. 2**), the GAG measured within the cell culture media surrounding each construct (measured every 3-4 days) accumulated to roughly equal levels as the static culture group. The GAG measured in dynamic constructs was roughly 40-70% that of human annulus tissue, depending on the age and anatomical location within the disc space. Mechanical

properties were also higher for shaken constructs at 4 weeks compared to free swelling controls (**Fig. 3**).

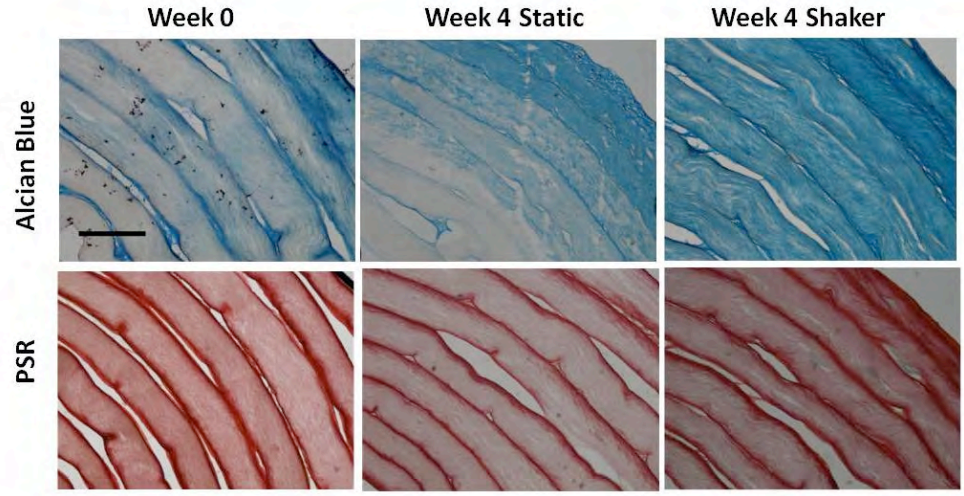

Figure 1: Histology of DAPS samples sectioned throughout the specimen midline and stained with either Alcian Blue or Picrosirius Red (PR). Scale = 500 µm.

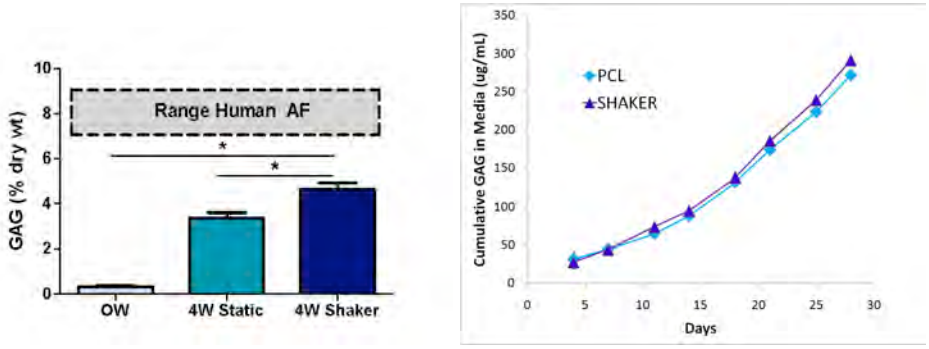

Figure 2: (Left) GAG content, reported in % dry weight (%DW). *=p<0.05 static compared to dynamic groups and both groups at 4 weeks compared to 2 weeks. Dash-lined box indicates native human AF benchmarks. (Right) GAG measured periodically in media for static and dynamic groups over 4 weeks.

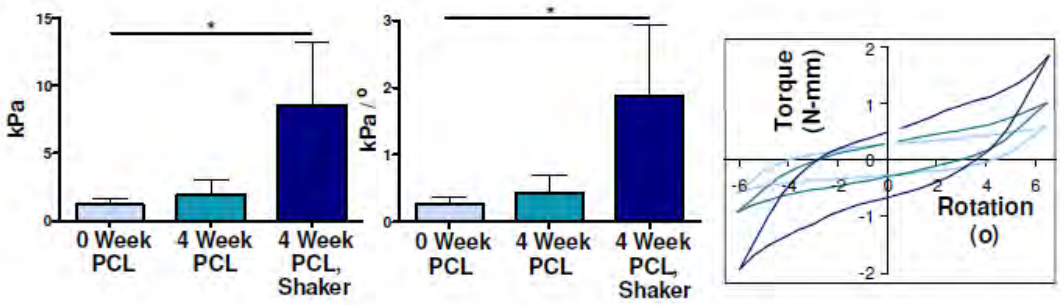

Figure 3: Torsional stiffness (left) and range of torque (center), n=4/group. (Right) Representative rotation-torque response of DAPS with time in culture. * = p≤0.05 compared to 0 week.

This study demonstrated the beneficial effects of dynamic culture on the maturation of MSC-laden DAPS at a length scale of the full intact tissue. This is the first study to our knowledge

showing beneficial effects of fluid mixing in the context of multi-lamellar electrospun mats tested using physiologically-relevant strategies (i.e. torsional mechanics). The increased levels of GAG incorporated across the lamellar space, while maintaining GAG deposits into the media, suggests that GAG produced by these MSCs positively responds to the culture environment and is free to migrate, helping to produce a more mature fibrocartilaginous matrix. However, since our biochemical and mechanical characterization suggested that our engineered disc falls short of several native tissue benchmarks, we continued to pursue options such as longer culture durations and options to increase the porosity of nanofibrous mats in order to promote enhanced inter-lamellar intra-lamellar organized ECM. This additional work is detailed below. Importantly, this early work established all methodologies required for the formation and culture of the angle-ply portion of the DAPS. Moreover, we demonstrated biomechanical and biochemical maturation of the AF construct as proposed. The finding that mechanical stimulation (via orbital shaking) improved growth suggests that our implanted DAPS structure might similarly benefit form fluid flow induced by loading after implantation.

Optimization of the Tissue Engineered NP Region:

In a second study in furtherance of the completion of this Aim, we examined the effect of transient exposure to chondrogenic medium to address the duration and time course that best establishes the NP and AF cell phenotype. Our focus here was on the formation and maturation of the mesenchymal stem cell (MSC) based nucleus pulposus (NP) region of our DAPS construct. This work was published as an abstract at the 2011 ASME Summer Bioengineering Conference in Nemacolin Woods, PA. The title of the abstract was: **Transient exposure to TGF-ß3 improves the functional properties of MSC-seeded photocrosslinked hyaluronic acid hydrogels** by authors Minwook Kim, Isaac E. Erickson, Jason A. Burdick, and Robert L. Mauck. A paper on this topic (with the same title and author list) was also published in the *Journal of the Mechanical Behavior of Biomedical Materials* in 2012.

To carry out this study, MSCs were isolated from tibial bone marrow, expanded in culture through passage 2-3, and seeded (60 million cells/mL) in 1% w/v photocrosslinkable HA (Lifecore Biomedical) as in our preliminary studies. Cylindrical MSC-based NP constructs (Ø4 × 2.25mm) were cultured in a chemically defined medium (1mL/construct). Constructs were then exposed to TGF-b3 at several different concentrations and durations, and compared to continuous exposure of TGF-ß throughout the culture period. Note, these doses and timings were expanded slightly from that proposed to better capture the full range of possible dosing schemes. The TGF-b3 dose was varied from the standard concentration (10ng/mL), to a high dose (50ng/mL), or to a very high dose (100ng/mL). For these higher concentrations, exposure times were limited to 3 or 7 days, with media changed one time over the first week. For the lower dose, exposure was for 3, 7, 21, or 42 days. A total of 8 groups were thus evaluated (10-cont, 10-21d, 10-3d, 10-7d, 50-3d, 50-7d, 100-3d and 100-7d), where the first number indicates dose, and the second number indicates duration. Media was changed twice weekly for the duration of study. Cell viability was assessed with Live/Dead staining (Invitrogen). Unconfined compression testing was carried out to determine construct dynamic and equilibrium properties. Total dsDNA, sulfated glycosaminoglycan (s-GAG), and collagen content was determined after papain digestion. Paraffin embedded sections (8µm) were stained with Alcian Blue for proteoglycan (PG) and Picrosirius Red for collagen. Significance was determined by two-way ANOVA with Tukey's post hoc test ($p<0.05$).

In this study, we determined that MSCs in our NP-like hydrogel regions were viable and biosynthetically active in HA under every condition. Constructs were geometrically stable with time (**Fig. 4A**), an important consideration for these NP analogs. Conversely, transient exposure to TGF-b3 altered construct biochemical and mechanical properties, depending on the dose and

duration of exposure. DNA content for most groups decreased with time, with the lowest levels found with the lower doses and shorter exposure times (not shown). Alternatively, GAG content significantly increased with time in every condition. Interestingly, several groups (i.e., 50-7d, 100-3d and 100-7d) produced GAG levels comparable to that of the control group (10-cont) (**Fig. 4B**). Collagen content at week three and six appeared independent TGF-b3 (not shown). Consistent with the increasing GAG content, construct mechanical properties increased with time in culture. By 6 weeks, the equilibrium modulus of the 100-7d grouped reached ~300 kPa, a level matching that of the 10-cont control group (p=0.169). Of note, it was necessary for this very high dose to be present for a full week to exert its effect, as the 100-3d group achieved much lower properties. The intermediate dose applied over 1 week (50-7d) also provided competitive mechanical properties compared to continual exposure or a single dose at the highest level (100-3d) (**Fig. 4C**). Histological evaluation showed that minimal PG was deposited with low doses of TGF-b3 applied for short periods of time. Conversely, very short exposures (one week or less) at higher doses produced staining comparable to that seen for continuous exposure at the lower doses (**Fig. 5**).

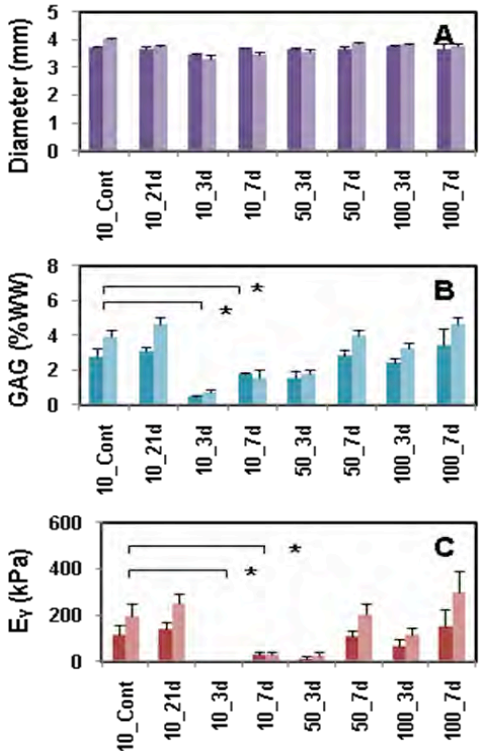

Figure 4: Biochemical and mechanical analysis. (A) Diameter (mm), (B) GAG (% wet weight, ww), (C) Equilibrium Modulus (kPa); N=5/group, Darker = 3w, Lighter = 6w, *p<0.05).

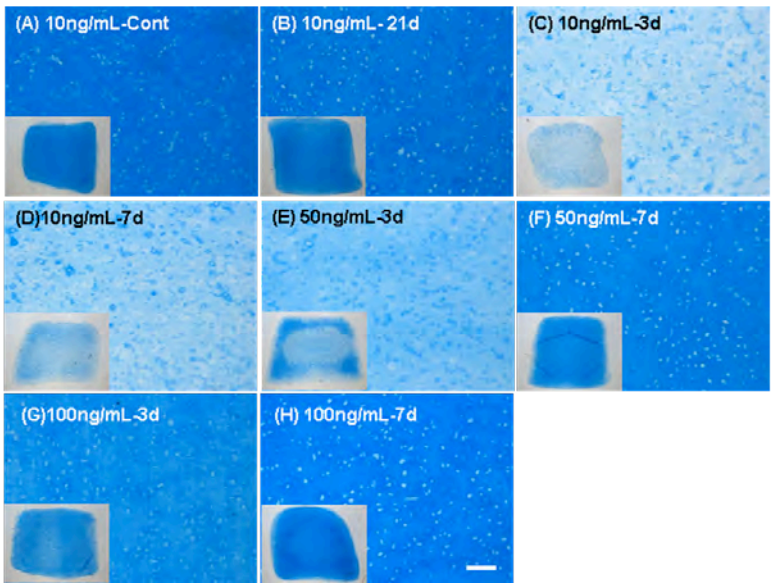

Figure 5: PG staining of constructs at 6 weeks after transient exposure to TGF-ß3 (inset: whole construct). Scale bar = 100 microns.

These findings showed a significant impact of TGF-b3 dose and duration of exposure on the functional maturation of MSC-laden HA hydrogels for NP engineering. Our results show that several dose and duration combinations can produce functional NP-like materials, and in some cases do so to a greater extent than continual exposure to lower concentrations. For example, in the most auspicious condition (100 ng/mL, exposure for 7 days), constructs increased in mechanical properties and biochemical content, reaching an equilibrium modulus of >300 kPa and ~5% GAG (per wet weight) after just 6 weeks. These mechanical properties were as high as those in the continual exposure group. This finding confirms that a robust and persistent NP-like state can be induced with very short exposure durations to this morphogen. Our findings point to the translational potential of this system, where a finite dose of TGF need only be delivered for a short period of time before implantation. Ongoing work in this area is exploring the maturation of this NP conjoined with the AF as described above, and under these growth factor and dosing regimens. Additional ongoing studies are challenging these constructs with serum after the differentiation has occurred, to mimic the transition to the in vivo space.

In addition to this work on the NP regions seeded with MSCs, we also carried out a study to examine the growth of engineered NP constructs based on NP cells derived from native tissue (as an alternative to MSCs). Towards restoring the NP, a number of biomaterials have been explored for cell delivery. These materials must support the NP cell phenotype while promoting the elaboration of an NP-like extracellular matrix in the shortest possible time. Our previous work with chondrocytes and mesenchymal stem cells demonstrated that hydrogels based on hyaluronic acid (HA) are effective at promoting matrix production and the development of functional material properties. However, this material had not been evaluated in the context of NP cells.

Therefore, to test this material for NP regeneration, bovine NP cells were encapsulated in 1% w/vol HA hydrogels at either a low seeding density (20 x 10^6 cells/ml) or a high seeding density (60 x 10^6 cells/ml), and constructs were cultured over an 8 week period. Outcome assays for this study were similar to those noted above, with the addition of quantitative real time PCR for markers of the NP phenotype. These engineered NP cell-laden HA hydrogels showed sustained

cell viability and functional matrix accumulation with increasing matrix content and mechanical properties with time in culture at both seeding densities (**Figs. 6-9**).

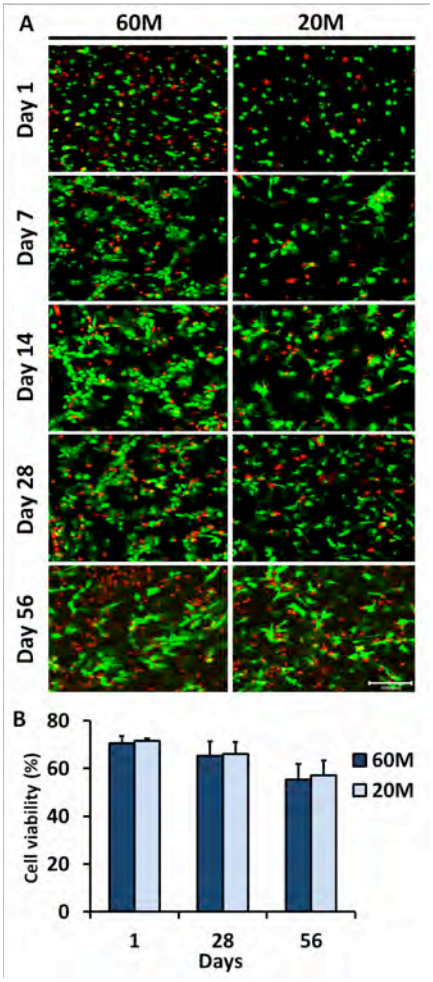

Figure 6: A) LIVE/DEAD staining of NPC-seeded HA constructs on days 1, 7, 14, 28 and 56 after encapsulation at either 60M or 20M seeding density (20X magnification, scale bar: 100 μm). B) Quantification of NPC viability in HA constructs on days 1, 28 and 56.

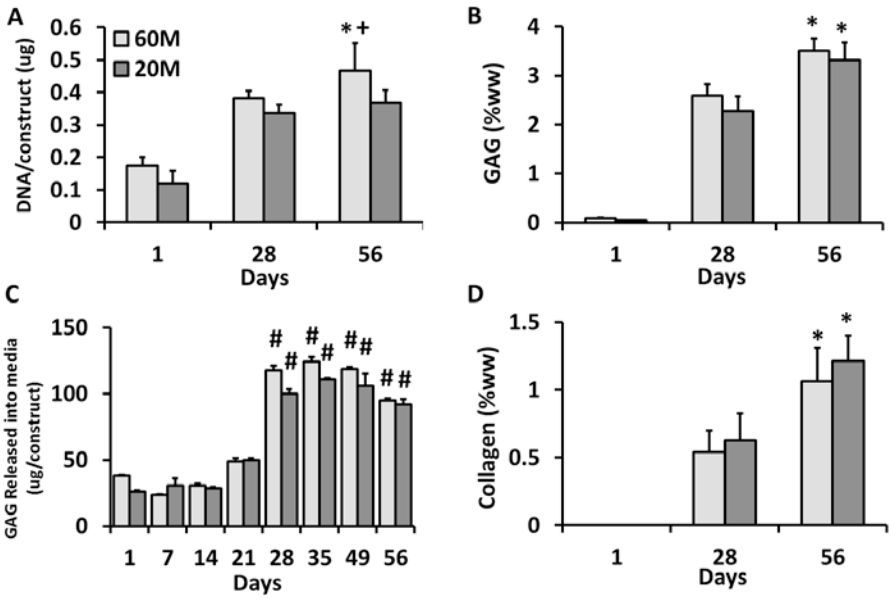

Figure 7: Biochemical composition of NP cell seeded HA constructs at seeding densities of 60M (grey) and 20M (dark grey) after 1, 28, 56 days of in vitro culture. A) DNA content per construct, n=5. B) GAG content per wet weight, n=5. C) GAG released to the media (per construct per day), n=3. D) Collagen content per wet weight, n=5. (* indicates $p < 0.05$ vs. day 28 within same group; + indicates $p < 0.05$ vs. 20M; # indicates $p < 0.05$ vs. day 21 within same group).

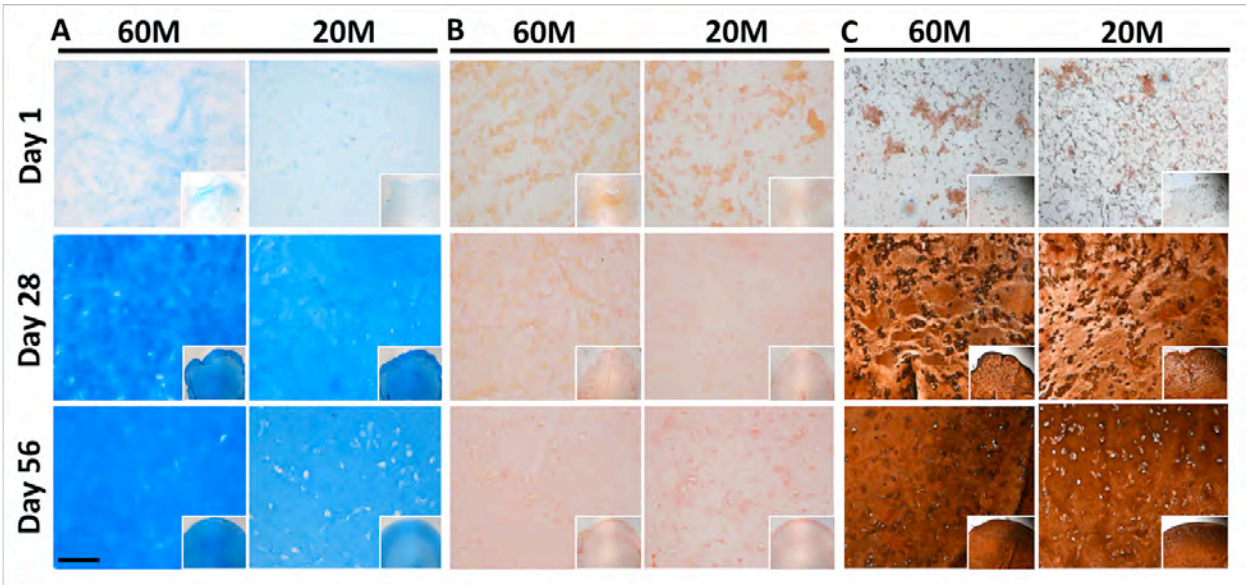

Figure 8: Matrix deposition in NPC-seeded HA constructs as a function of culture duration and seeding density. (A: Alcian blue staining of proteoglycans, B: Picrosirius red staining for collagens, C: immunostaining for collagen type II; 10× magnification (inset: 5×), scale bar: 100 µm).

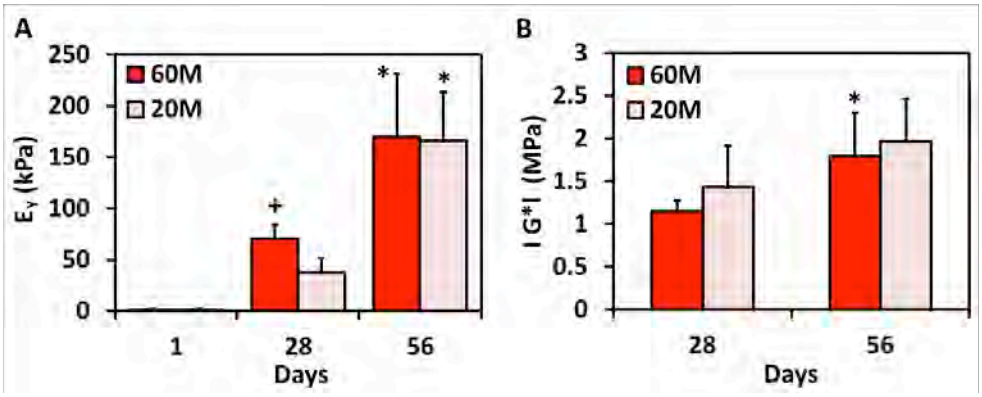

Figure 9: Equilibrium compressive modulus (A) and dynamic compressive modulus (B) of NPC-seeded HA constructs over 8 weeks of in vitro culture (*indicates $p < 0.05$ vs. at day 28; $^{+}$indicates $p < 0.05$ vs. 20M group, n=4~5/group/time point).

Furthermore, encapsulated cells showed NP-specific gene expression profiles that were significantly higher than monolayer expanded NP cells, suggesting a restoration of the NP phenotype (**Fig. 10**). Interestingly, these levels were higher at the lower seeding density compared to the higher seeding density.

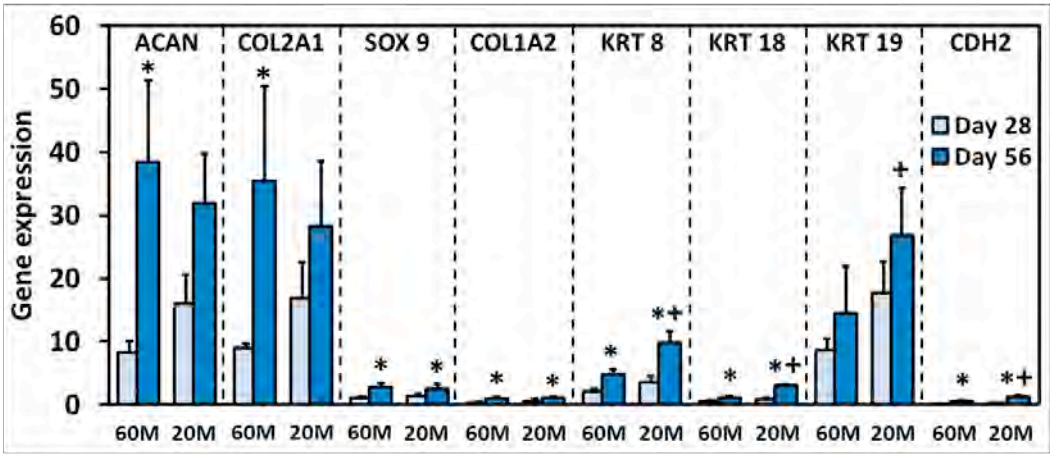

Figure 10: Expression of aggrecan (ACAN), collagen II (COL2A1), SOX 9, collagen I (COL1A2), cytokeratin (KRT) 8, 18, 19, and N-cadherin (CDH 2) after 28 and 56 day of culture for NPC-seeded HA constructs. Expression levels were normalized to glyceraldehyde 3-phosphate dehydrogenase (GAPDH) and expanded NP cells prior to encapsulation (* indicates $p < 0.05$ vs day 28; + indicates $p < 0.05$ vs 60M). (n=3/group/time point)

These findings support the use of HA-based hydrogels for NP tissue engineering and cellular therapies directed at restoration or replacement of the endogenous NP. This work was published as several abstracts and a full length manuscript in *Acta Biomaterialia* in 2015, as: **Phenotypic Stability, Matrix Elaboration, and Functional Maturation of Nucleus Pulposus Cells Encapsulated in Photocrosslinkable Hyaluronic Acid Hydrogels** by authors Dong Hwa Kim, John T. Martin, Dawn M. Elliott, Lachlan J. Smith, and Robert L. Mauck.

Optimization of a Full DAPS Construct Composed of an Engineered AF and an Engineered NP Region:

To complete the in vitro development of our tissue engineered disc, we recently finished a series of studies in which the polymer nanofiber based AF and the hydrogel NP were combined together to form a full DAPS structure. In this study, we defined the in vitro growth trajectory of DAPS seeded with AF and NP cells or MSCs over a 15 week period. As part of this same work (and described in the work associated with Aim 3 below), we then tested their ability to integrate and function after implantation in the rat tail after short and long-term preculture periods.

To carry out this study, poly(ε-caprolactone) (PCL) nanofibers were electrospun onto a rotating mandrel as aligned fibrous sheets (th=250μm). Strips were excised at 30^{o} to the fiber direction and two strips with alternating ±30^{o} alignment were wrapped concentrically to form the AF. These were fabricated with one layer (th=125μm) of poly(ethylene oxide) for every two layers of PCL (th=125 μm) to improve initial cell colonization. Formed AF regions were sterilized in ethanol, coated with fibronectin and seeded directly with either bovine AF cells or bovine MSCs (2M cells/construct). Methacrylated hyaluronic acid (MeHA) was produced by reacting HA with methacrylic anhydride. A photocrosslinkable 1% w/v solution was produced by dissolving MeHA and 0.05% Irgacure 2959 in phosphate-buffered saline. Bovine NP cells or bovine MSCs were suspended in the MeHA solution (20M cells/mL, 600K cells/construct), which was poured into a mold and photo-polymerized with UV light. AF and NP regions (n=4/group) were cultured separately in chemically defined media containing TGFβ3 and then combined at 2 weeks. At regular intervals over 15 weeks, the elastic and viscoelastic mechanical properties, glycosaminoglycan (GAG) and collagen content, and alcian blue (proteoglycan, PG) and picrosirius red (collagen) staining, were evaluated.

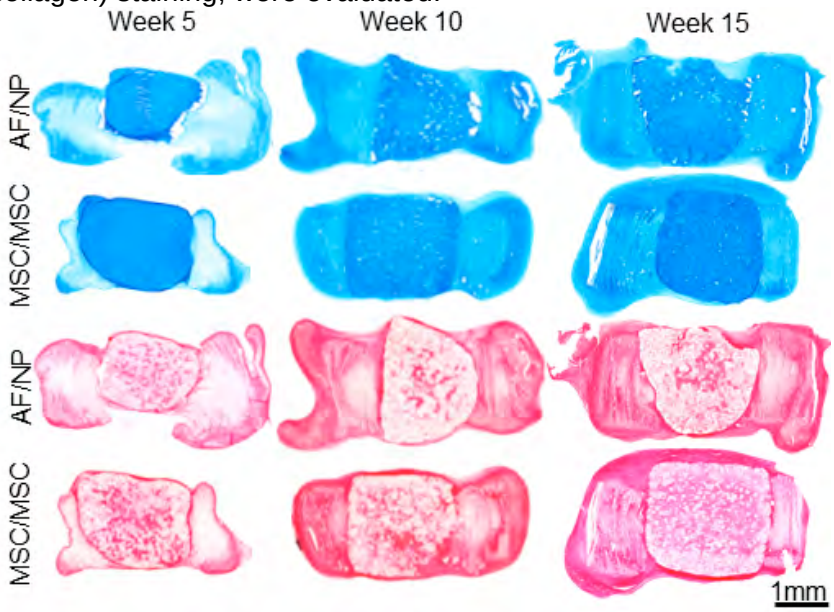

Figure 11: Alcian blue (top rows) and picrosirius red (bottom rows) of AF/NP and MSC/MSC DAPS over 15 weeks of culture.

Results from this study showed that both MSC- and disc cell-seeded DAPS matured compositionally and functionally over time in culture (**Fig. 11**). Collagen- and PG-positive staining initiated at the periphery of the AF at 5 weeks that gradually infiltrated to deeper regions by 10 weeks. At 15 weeks, a peripheral concentration of dense extracellular matrix indicated encapsulation. Both collagen and PG-positive staining in the NP increased over time, with

collagen staining nucleating at the center of the NP, and PG staining evenly distributed throughout the NP. Measurements of GAG and collagen (**Fig. 12a**) indicated that there was a consistent increase in matrix deposition in the AF and NP regions for both cell types, with production by MSC-seeded DAPS outpacing that of disc-cell seeded DAPS. There were no significant changes in elastic mechanical properties (toe and linear region compressive moduli) over 15 weeks, and no mechanical differences between MSC and disc cell-seeded DAPS (**Fig. 12b**). There was a significant increase in creep strain over the first 10 weeks that plateaued from 10 to 15 weeks, with no differences between cell types (**Fig. 12b**).

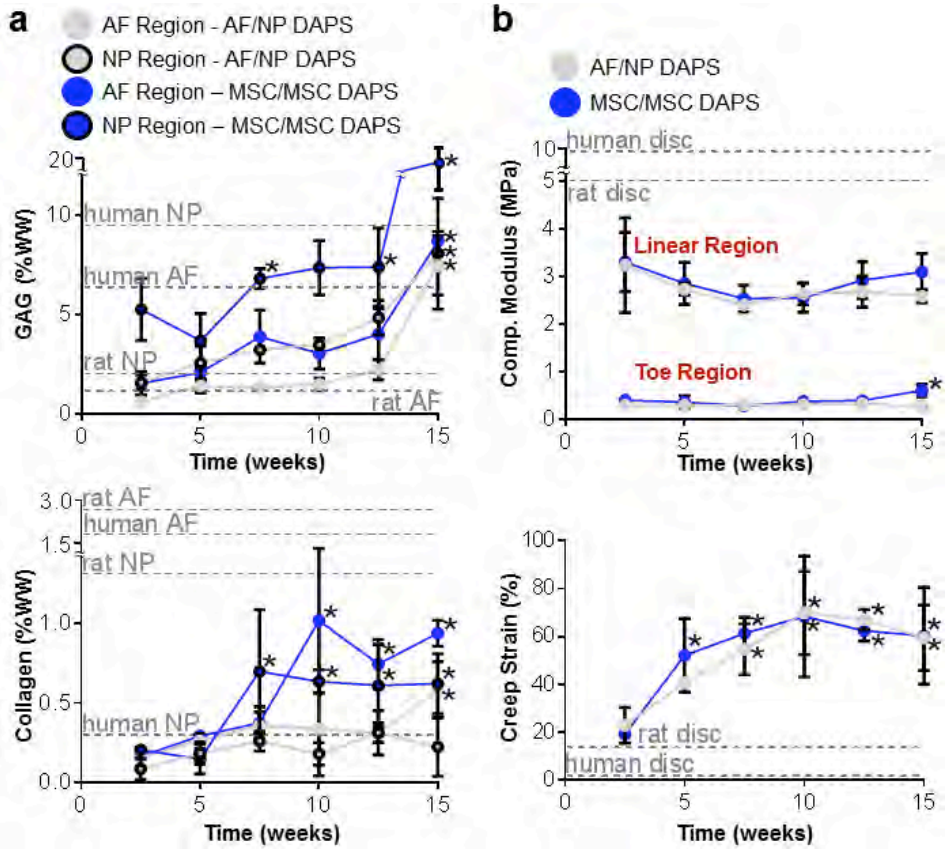

Figure 12: (a) GAG and collagen content, and (b) compressive moduli and creep strain of DAPS over 15 weeks of culture. *, $p<0.05$ vs. week 2.5. Rat, human values from the literature.

This study demonstrated that an engineered disc composed of an electrospun AF and a hydrogel NP matured compositionally and functionally with time in culture. With extended in vitro growth, the compositional and functional properties of disc constructs reached levels that were comparable to native tissue from both human and rat. GAG content of MSC/MSC and AF/NP seeded DAPS approached human levels in the AF and NP regions, while collagen content was 40% of the human AF and exceeded or matched that of human NP. The DAPS constructs showed nonlinear stress/strain behavior and moduli that were within 70% of the native rat disc; however, creep strain exceeded native levels. Thus, while DAPS resembled native tissue in terms of their elastic mechanical behavior, there were differences in time dependent mechanisms, perhaps driven by differences in the ability to retain water under load, or by plastic deformations in the AF region. The most sensitive metrics of implant maturity appeared to be collagen content and creep strain, both of which peaked at 10 weeks. These findings were submitted for publication at the Summer Bioengineering, Biotransport, and Biomechanics Meeting and a full length manuscript is now in preparation. The title of this work

is **In Vitro Growth Trajectory and In Vivo Implantation of Cell-Seeded Disc-like Angle Ply Structures for Total Disc Replacement** with authors John T. Martin, Dong Hwa Kim, Kensuke Ikuta, Christian G. Pfeifer, Lachlan J. Smith, Dawn M. Elliott, Harvey E. Smith, Robert L. Mauck.

Based on the results of these studies, all portions of Aim 1 have thus been completed per our original statement of work.

Aim 2: Implant the tissue engineered DAPS in a subcutaneous environment after varying period of in vitro pre-culture and evaluate maturation using the same assays and evaluation criteria as in Aim 1.
Aim 3: Implant the tissue engineered DAPS in situ using a rat tail disc replacement model. Evaluate DAPS maturation and in situ integration under static conditions and with resumption of mechanical loading. The engineered DAPS will be evaluated under two fixation conditions: an Immobilization group and Compression group, which is loaded axially with 0.5X body weight. Both of these fixation conditions will be applied for either short duration (8 weeks, followed by release and an additional 8 weeks normal loading) or held for the entire study duration (16 weeks). Structure, mechanics, and composition of the functional DAPS and its interface will be evaluated at 2, 8, and 16 weeks. Both fixation conditions will be compared against a sham control in which all surgery and fixation conditions are the same, but without disc removal or DAPS placement.

Given that Aims 2 and Aim 3 are both in vivo portions of the project, and so are related to one another, we will describe our accomplishments in these Aims together. Most of the work accomplished relates to the more challenging Aim 3, the implantation into the actual disc space. This Aim represented the culmination of our project. The work focused on these Aims has been substantially completed over the last three years of funding (Years 2&3 plus no-cost extension year). Note that deviations from the stated goals were necessary at times to further the experimental goals and based on the experimental findings, as will be described below.

Development of an Engineered Disc Implantation Model in the Rat Caudal Spine:
Our first step in this work was pilot surgeries (with a few acellular DAPS) to establish the eventual implantation of the fully matured versions developed in later stages of the project. Specifically, we started by developing and validated the surgical technique for implantation of the tissue engineered disc into the rat caudal disc space. The surgical technique was designed to be minimally invasive in order to prevent vascular damage and promote rapid healing. Three surgical groups were evaluated: sham, discectomy and implantation of acellular disc constructs. Healing and integration were evaluated at time points up to one month using histology and microCT. At one week, histological evaluation showed the construct well placed in the disc space (**Fig. 13**), with lamellar architecture characteristic of the native tissue. At subsequent time points however, histology showed migration of the construct out of the disc space, and microCT (**Fig. 13**) suggested the disc space had subsequently collapsed.

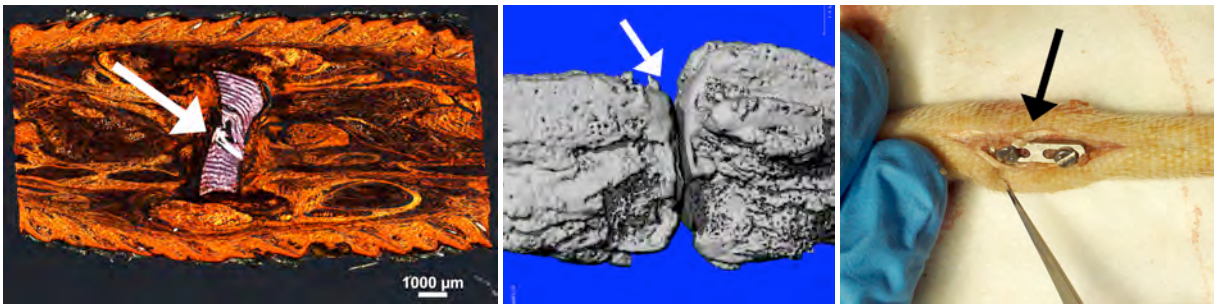

Figure 13: Left. Histology showing acellular disc implant (arrow) at 1 week. Middle. MicroCT showing collapsed disc space (arrow) at 4 weeks. Right. Original internal fixation device to (arrow) to stabilize joint and retain implant in disc space.

To overcome this problem of disc collapse, we designed a series of internal and external fixation devices to stabilize the disc space in the immediate post-implantation time period. The goals of these designs were to enhance retention of the construct in the disc space and stabilize the joint during healing. Indeed, these early findings led to our next major time investment – improving implant stability and improving infiltration and anchorage of the implant via the ingrowth of endogenous cells in the disc environment. This work was published in 2014 in *Acta Biomaterialia* under the title **Translation of an Engineered Nanofibrous Disc-like Angle Ply Structure for Intervertebral Disc Replacement in a Small Animal Model** with authors John T. Martin, Andrew H. Milby, Joseph A. Chiaro, Dong Hwa Kim, Nader M. Hebela, Lachlan J. Smith, Dawn M. Elliott, and Robert L. Mauck, as well as at several conference abstracts.

In brief, this work built from our development of disc-like angle ply structures (DAPS) consisting of layered, oriented electrospun scaffold forming a concentric annulus fibrosus (AF) coupled with a hydrogel nucleus pulposus (NP). Based on early studies wherein DAPS were implanted into the rat caudal spine, approximately half of the implants were displaced, and for those that remained in place, there was limited cell infiltration into the dense scaffold. To address this, this study evaluated an external fixator to improve implant retention by stabilizing the rat caudal spine and tested a new DAPS design wherein sacrificial layers were included to improve cell infiltration and anchorage by endogenous cells.

To carry out this study, poly(ε-caprolactone) (PCL) nanofibers were electrospun onto a rotating mandrel as aligned fibrous sheets (th=250µm). Strips were cut 30^{o} to the fiber direction and two strips with alternating $\pm 30^{o}$ alignment were wrapped concentrically to form the AF region of the DAPS (**Fig. 14**, top left and top right). DAPS with sacrificial layers (sDAPS) were fabricated with one layer (th=125µm or 250µm) of poly(ethylene oxide) (PEO, water soluble and rapidly degrading) or 75:25 poly(lactic-co-glycolic acid) (PLGA, slowly degrading) for every two layers of PCL (th=125 µm). Final dimensions were: OD=5mm, ID=1 mm, height=2 mm. To determine if cell infiltration is improved by including sacrificial layers, sDAPS were seeded with bovine AF cells and cultured for 28 days. First, sDAPS (with PEO) were washed to remove PEO, lyophilized and coated overnight in 20 µg/mL fibronectin. Then, bovine AF cells were seeded onto top and bottom surfaces ($2x10^{6}$ total cells), and sDAPS were cultured in serum-containing media. Infiltration was assessed via DAPI staining. An external fixator was designed to unload and stabilize the rat caudal spine (**Fig. 14**, bottom left and bottom right). Surgical wires were passed laterally through the mid-height of vertebrae adjacent to the C8/C9 disc, and the fixator was applied leaving access to the dorsal tail. A dorsal incision was made, the native disc was removed and AF-only DAPS or sDAPS were implanted into the disc space (DAPS: 14 days (n=4), 28 days (n=5), sDAPS: thin PEO, thick PEO, thin PLGA and thick PLGA, 14 days

(n=3/group)). An additional discectomy control group (14 days (n=4), 28 days (n=4)) and external fixator plus discectomy control group (14 days (n=2), 28 days (n=4)) were included to verify disc height preservation with fixation. Rat tails were imaged longitudinally with a fluoroscope to quantify disc height index (DHI). Then, following euthanasia, tails were imaged via μCT to assess adjacent bone remodeling. Finally, histological sections were stained with H&E and imaged in bright field or polarized light, or stained with DAPI and imaged in fluorescent light.

Results from this study showed that disc height was preserved by external fixation, even after total discectomy. At days 14 and 28, the fixator+discectomy and fixator+DAPS DHI were not different from immediate post-operative values (**Fig. 14**). μCT confirmed that fixation prevented disc space collapse, with minimal superficial bone remodeling at the wire insertion sites (**Fig. 15**). In addition, all DAPS implanted with fixation remained in the disc space and maintained their lamellar architecture (**Fig. 15**). sDAPS maintained interlayer gaps, enabling cell infiltration into the lamellar structure both in vitro and in vivo. In in vitro studies, AF cells penetrated the full height of both thick and thin layer PEO sDAPS after one week, and proliferated, filling the lamellar structure over 28 days (**Fig. 16**). PCL-only DAPS were poorly infiltrated, with central areas completely devoid of cells. When implanted in vivo, sDAPS remained in place and maintained their structure over time. Matrix deposition between layers was evident for both thin and thick layer PEO sDAPS, and appeared more rapidly than in PLGA sDAPS, though PLGA sDAPS better maintained their structure during implantation (**Fig. 16**). While some matrix deposition was apparent in thin PLGA sDAPS, thick PLGA sDAPS were not infiltrated by cells, as the implant was encapsulated by fibrous tissue before PLGA degraded.

This study advanced the development of an engineered disc for total disc replacement. We established a viable in vivo model by stabilizing the rat caudal spine and improved DAPS by including routes for cell migration. These findings demonstrate that application of an external fixator preserves disc height and markedly improves retention of the DAPS. A previous study had shown that a disc comprised of a collagen AF and an alginate NP was retained in the rat tail without fixation. This may be due to differences in the surgical approach or the physical properties of the construct, however, with the external fixation developed herein, one can implant constructs with a range of physical properties and protect implants for a defined period after surgery. PCL-only DAPS were poorly infiltrated by cells, a common drawback of electrospun scaffold. Rapidly degrading layers of PEO allowed colonization of the DAPS by cells that secreted extracellular matrix, while slowly degrading layers of PLGA marginally improved infiltration. This suggests that early migration of endogenous cells will be important for integration. These data established the rat caudal spine (stabilized by external fixation) as a test bed to assess long term implant biocompatibility and, in addition, that sacrificial layers in the DAPS AF region improve implant patency and subsequent cell infiltration.

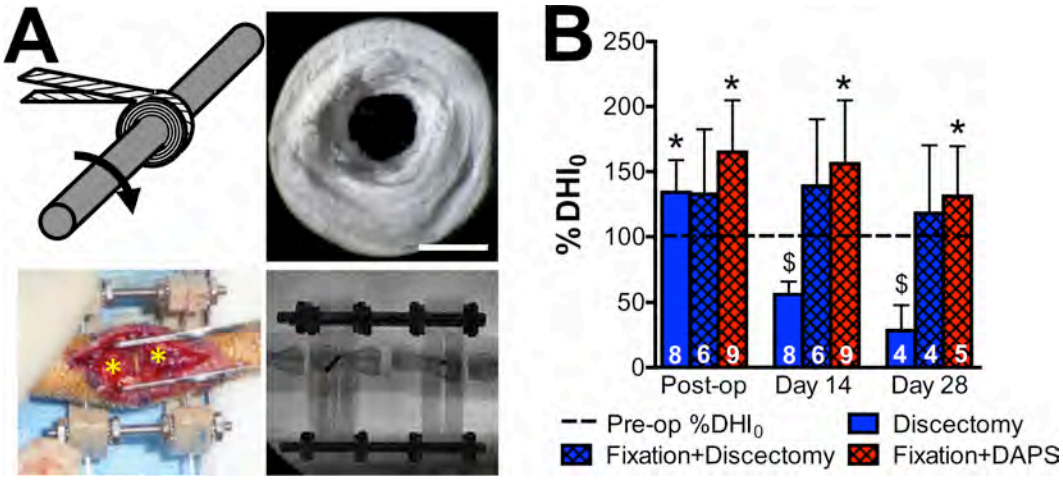

Figure 14: (A, top left and top right) DAPS were fabricated by wrapping strips of electrospun PCL with alternating alignment into concentric layers, scale=2mm. (A, bottom left) An external fixator was used to stabilize adjacent caudal vertebrae (asterisk). (A, bottom right) The fixator was radiolucent by design to enable disc height quantification. (B) Disc height index (DHI). Sample number is indicated on each column, *, $p<0.05$ from pre-op and $, $p<0.05$ from all other groups.

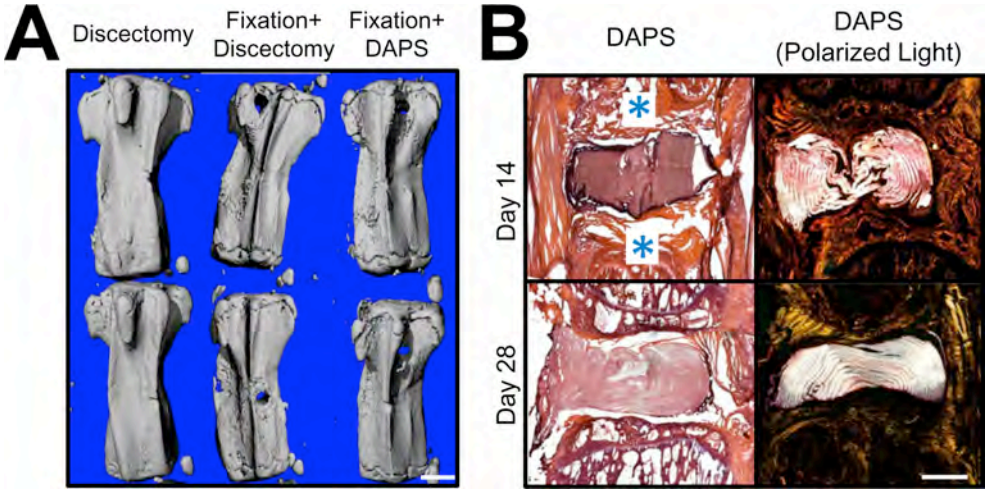

Figure 15: (A) μCT reconstructions after 28 days in vivo, scale=2mm. (B) H&E-stained DAPS in brightfield and polarized light after 14 or 28 days in vivo, scale=1mm. Vertebrae are marked with an asterisk.

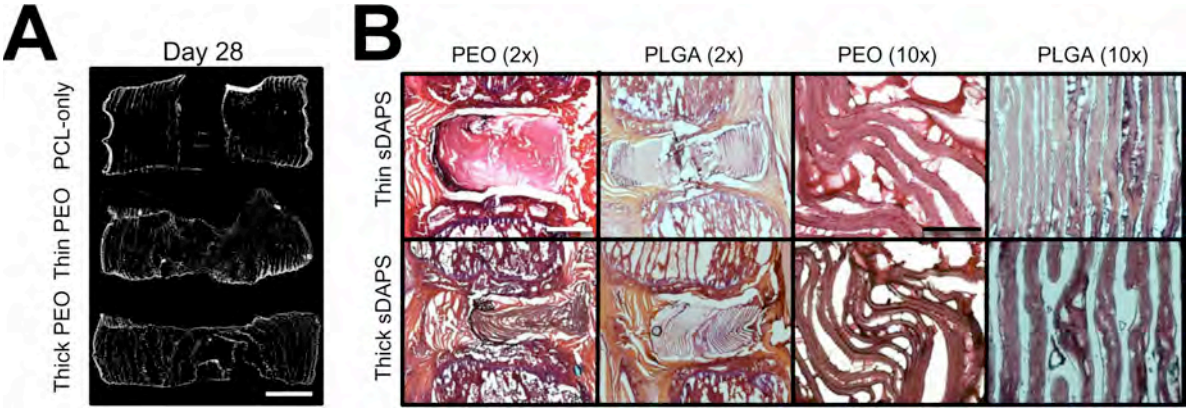

Figure 16: (A) DAPI-stained DAPS after in vitro culture for 28 days, scale=1mm. (B) Low and high magnification H&E-stained sDAPS after 14 days in vivo, scale: 2x=1mm, 10x=500μm.

Development of an Radio-opaque Implants to Monitor Position Non-Invasively:

Given that implant migration was a potential problem in this rat tail model, we also developed methods to non-invasively image and monitor implant position as a function of fixation. To do so, we developed a radiopaque nanofibrous scaffold by electrospinning a polymer/heavy metal salt solution, and used this material as a diagnostic tool for model development. In this study, we characterized the radiopacity, structure and mechanical behavior of the scaffold, and showed its utility in an *in vivo* model of intervertebral disc replacement. This work was published in abstract form at the 2014 Orthopaedic Research Society Meeting and a full length manuscript titled **A Radiopaque Electrospun Scaffold for Engineering Fibrous Musculoskeletal Tissues: Characterization and *In Vivo* Application** with authors John T. Martin, Andrew H. Milby, Subash Poudel, Kensuke Ikuta, Dong Hwa Kim, Christian G. Pfeifer, Harvey E. Smith, Dawn M. Elliott, and Robert L. Mauck is now in review.

To carry out this study, radiopaque scaffolds were generated from a 14.3% w/v slurry of poly(ε-caprolactone) (PCL) mixed with zirconium(IV) oxide (zirconia), a radiodense powder with a characteristic dimension <100 nm. Slurries were electrospun while continuously mixing, and collected onto a rotating mandrel to create an aligned nanofibrous sheet (th.=200μm). Four scaffold-types with varying radiodensity were fabricated: 100% PCL, 90% PCL/10% zirconia, 75% PCL/25% zirconia, 50% PCL/50% zirconia. Each scaffold was assayed for structural continuity, radiodensity and mechanical strength. To assess nanostructure, samples were imaged by SEM (n=1/group). To measure radiodensity, 8 mm diameter samples were punched from each scaffold and scanned by μCT (vivaCT 75, SCANCO) at 20μm resolution (n=5/group). The linear attenuation coefficient of each sample was calculated from volumetric reconstructions. Scaffold strips (5mm x 40mm) were tested in uniaxial tension in the fiber direction (n=5/group). The mechanical testing protocol consisted of a 0.05 N preload, followed by extension to failure at a rate of 0.1% strain/s. Tensile modulus was calculated as described previously.

Disc-like angle ply structures fabricated from radiopaque scaffold (rDAPS) were then implanted into the rat caudal spine. Strips were cut from aligned radiopaque scaffold 30 degrees to the fiber direction and two strips with alternating ±30 degrees alignment were wrapped concentrically to form the annulus fibrosus region of the rDAPS. To implant rDAPS, surgical wires were passed laterally through the mid-height of vertebrae adjacent to the C8/C9 disc, and an external fixator was applied (**Fig. 17**). A dorsal incision was made, the native disc was removed and rDAPS were inserted into the disc space. Rats were returned to cage activity and euthanized at 28 days. Two implant types were used in this study: a radiodense implant, “50/50 rDAPS” with 2 layers of 50% PCL/50% zirconia (n=2); a radiolucent implant,”75/25 rDAPS” with 1 layer of 75% PCL/25% zirconia, 1 layer 100% PCL and one layer of degradable 75:25 poly(lactic-co-glycolic acid) (PLGA, to provide a route for cell migration once degraded) (n=3). To monitor changes in implant position and structure *in vivo*, rat tails were imaged longitudinally with a fluoroscope. Then, following euthanasia, tails were imaged via μCT to assess implant structure and histological sections were stained with picrosirius red (for collagen).

Results from this study showed that we could create a trackable radio-opaque construct. SEM revealed that all formulations of radiopaque scaffold had continuous and aligned fibers (**Fig. 18**). Zirconia was embedded within fibers at lower concentrations, but at the highest concentration it was evident that zirconia aggregated into large pellets exterior to the fibers (**Fig. 18**). In addition,

as zirconia increased fiber diameter decreased. Scaffold modulus increased with ziroconia content, except at the highest concentration (**Fig. 18**). Scaffold radiation attenuation increased with zirconia content plateauing at 25% zirconia (**Fig. 18**); PCL alone had no signal and thus 3D reconstruction was not possible. Both formulations of rDAPS were visualized intra- and post-operatively. 50/50 rDAPS had a distinct signal (**Fig. 19**), more intense than that of the native bone, while the 75/25 rDAPS cast a radiolucent shadow similar to bone (**Fig. 19**). rDAPS remained in the disc space over 28 days with no change in position or shape. These results were confirmed by μCT; both types of rDAPS had a signal distinguishable from bone allowing for the reconstruction of each separately. Reconstructions of 50/50 rDAPS demonstrated that the radiopaque implants occupied the disc space and did not cause an adverse reaction (**Fig. 20**). 3D reconstructions of 75/25 rDAPS demonstrated that lamellar structure was intact after 28 days (**Fig. 19**). Images of histological sections confirmed that new collagen was deposited between layers, though the PLGA had not completely degraded (**Fig. 20**).

In this study, we developed and characterized a radiopaque electrospun scaffold composed of PCL, a standard tissue engineering polymer, and zirconia, a heavy metal salt. We demonstrated that scaffold radiopacity and mechanics can be tuned by altering the concentration of zirconia. In addition, we fabricated radiopaque implants and validated a rat caudal spine model of disc replacement. The radiation attenuation of each scaffold increased with zirconia content and plateaued at 25% zirconia. Radiopaque implants made with high and low concentrations of zirconia were visualized in the rat caudal spine. In addition, the radiopaque scaffold was compatible with the formation of new collagen by endogenous cells.

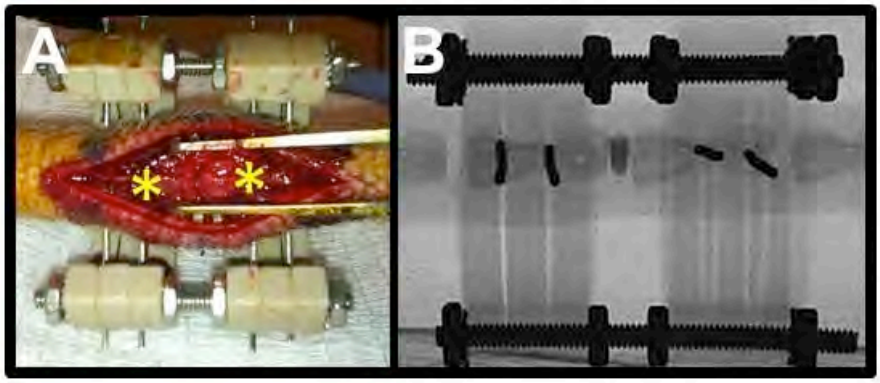

Figure 17: A) rDAPS were implanted between vertebrae (asterisk) of the rat caudal spine to demonstrate the utility of radiopaque scaffold. B) The vertebrae were stabilized with a radiolucent external fixator.

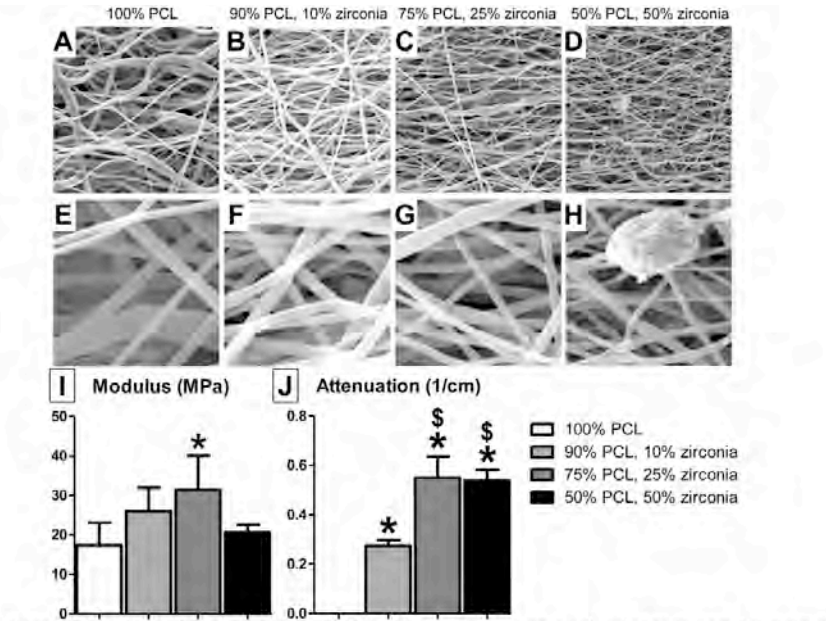

Figure 18: Characterization of radiopaque scaffold. SEM images at A-D) 2,000x magnification and E-H) 10,000x magnification, I) tensile modulus and J) linear attenuation.

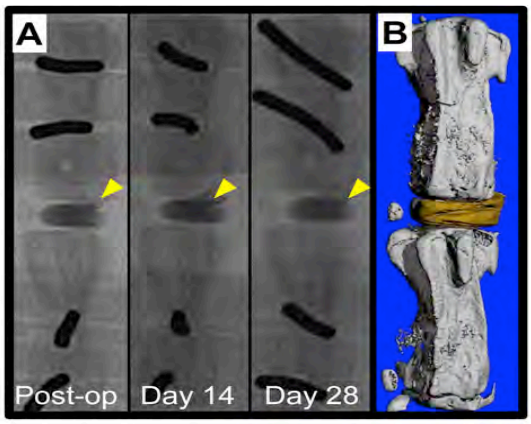

Figure 19: *In vivo* implantation of high radiodensity rDAPS. A) Fluoroscopy over 28 days. B) µCT reconstruction after 28 days.

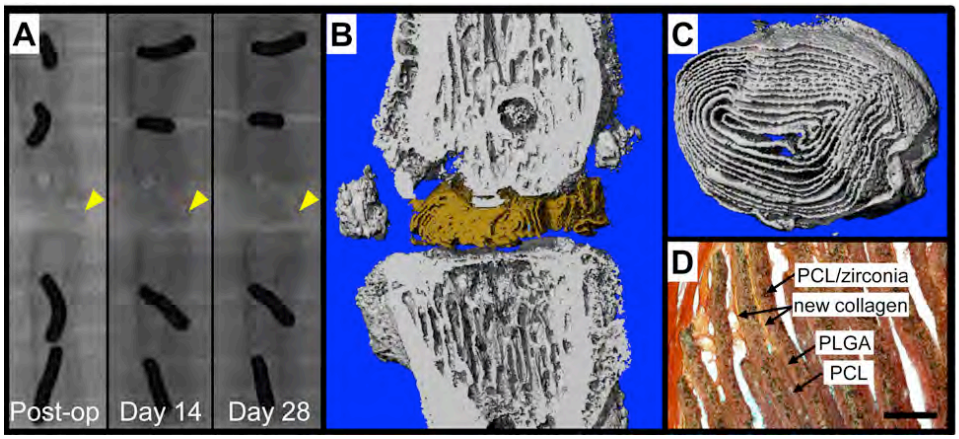

Figure 20: *In vivo* implantation of low radiodensity rDAPS. A) Fluoroscopy over 28 days. B) μCT reconstruction after 28 days. C) Reconstruction of scaffold only after 28 days. D) Picrosirius red-stained section at day 28.

Implantation and Evaluation of Pre-Matured Engineered Discs in the Rat Caudal Spine:

In the final series of studies in pursuit of Aim 3, engineered discs (n=6/group) consisting of AF/NP cell-seeded DAPS were implanted into the rat caudal disc space after preculture for 5 (immature) or 10 weeks (mature). Athymic retired breeder rats were prepared for implantation by installing a PEEK/stainless steel external fixator designed to unload and stabilize the caudal disc space as above. Two surgical wires were passed through the C8 and C9 vertebrae and the external fixator was mounted. Following a dorsal skin incision, the native C8/C9 disc was removed and constructs were implanted. Rats were returned to normal cage activity and euthanized 5 weeks after implantation. Vertebra-DAPS-vertebra segments were scanned by micro-CT, and sectioned and stained with alcian blue/picrosirius red for proteoglycans and collagens, respectively.

After implantation for five weeks, we observed no differences between immature and mature DAPS. Micro-CT scans revealed normal vertebra morphology, with some new bone deposition around the surgical wire holes (**Fig. 21**). Alcian blue/picrosirius red stained vertebra-DAPS-vertebra sections showed that DAPS maintained their structure after 5 weeks of implantation and integrated well into the adjacent soft tissue for both mature and immature implants. However, integration into the adjacent vertebra was less robust (**Fig. 21**). Furthermore, there was a marked loss in PG-positive stain in the NP in both groups, as is evidenced by the loss of blue staining in the NP region.

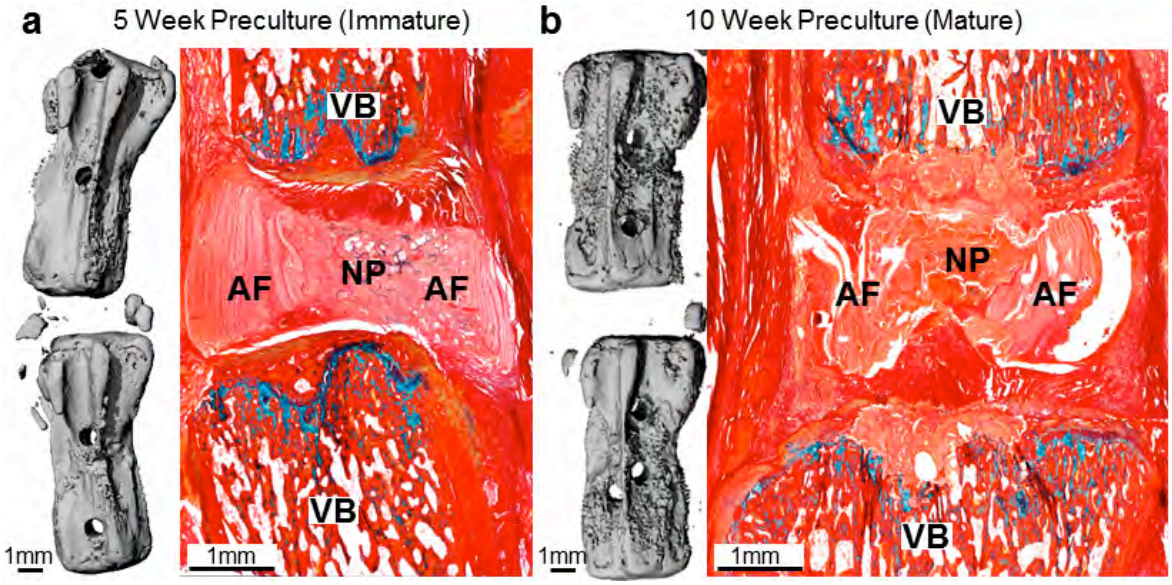

Figure 21: DAPS pre-cultured for (a) 5 (immature) or (b) 10 weeks (mature) evaluated by mCT and histology 5 weeks after implantation. AF - annulus fibrosus, NP - nucleus pulposus, VB - vertebral body.

Given the dramatic loss of proteoglycans in the NP, our next series of studies were focused on the short term, to determine precisely when this molecule was being lost. In related work, our team had developed T2-weighted MR imaging methods for the evaluation of structure and content of the disc, with a specific focus on changes in the NP that typify degeneration (Martin et al., *J Orthop Res*, 2015). We applied this analysis method to our implanted engineered discs

in harvested rat caudal spines (**Fig. 22**). MR imaging at 4.7T identified the disc structure of native disc well, where the T2 signal in the NP was quite high compared to the AF region. In vitro cultured engineered discs showed a similar pattern of T2 signal at 10 and 20 weeks of culture (not shown). Likewise, 3 days after implantation, the engineered disc morphology and T2 signal matched that of the native disc (**Fig. 22**). However, by 7 days post-implantation, a considerable amount of the T2 signal in the NP had been lost, consistent with our observation of a loss of NP proteoglycan at 5 weeks through histological analysis.

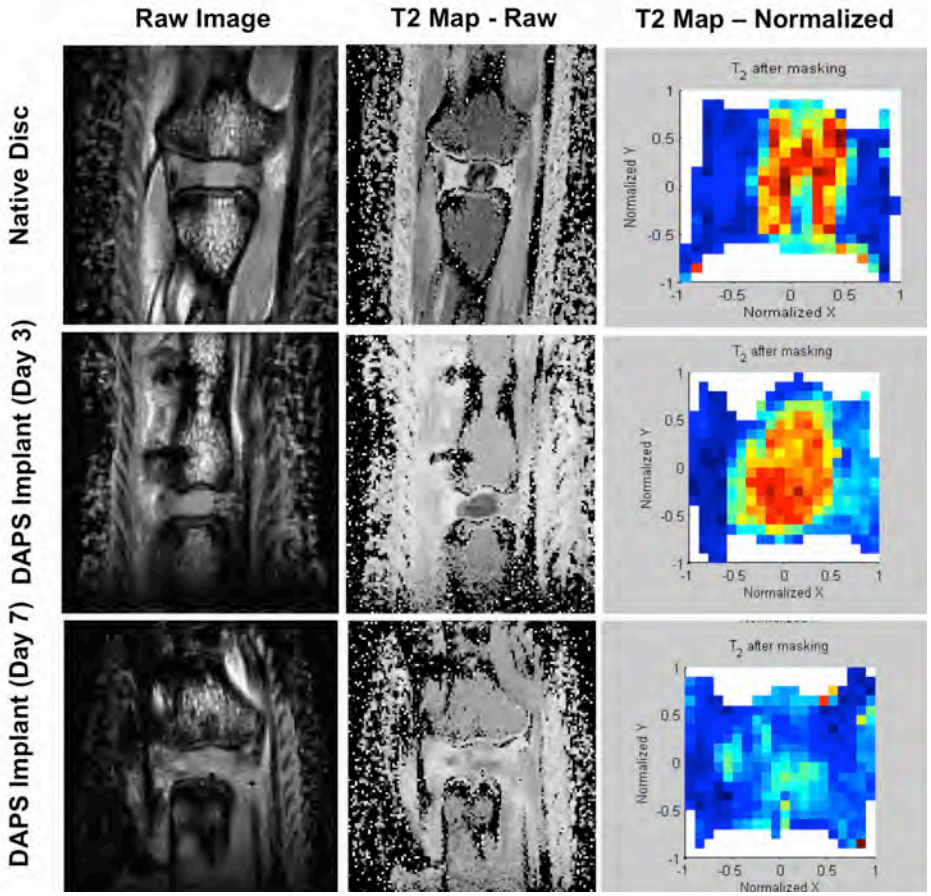

Figure 22: Raw MR images (first column) and T2-weighted (middle column) MR images and analysis of native (top row) and implanted tissue engineered constructs (middle and bottom row) in the rat caudal spine. Engineered discs (seeded with NP and AF cells) were pre-cultured for 5 weeks and implanted for 3 (middle row) or 7 days (bottom row). T2-weighted MRI imaging was performed at 4.7T on whole tails, and T2 values computed and plotted in a normalized grid.

Collectively, our in vivo data suggests that while DAPS retain their gross structure upon implantation, there was a marked depletion of PGs in the NP region. This suggests a shift in cell behavior when removed from the in vitro environment and placed in the in vivo disc space. As this loss of NP proteoglycan occurred regardless of whether the construct was seeded with native disc cells (NP and AF) or with MSCs, this suggests that the in vivo environment may be too taxing for the implant at this stage. Interestingly it did not seem to matter whether the engineered disc had matured for 5 weeks or for 10 weeks, suggesting that the amount of matrix deposited at the time of implantation did not serve a protective role. In very recent studies, to complete Aim 2, we implanted mature DAPS (10 weeks) and saw the same loss of proteoglycan

in the NP space over the course of 1 week (not shown). Such changes and may be related to the abrupt removal high concentration of media components such as glucose or TGFβ3 upon *in vivo* implantation. Alternatively, the highly inflammatory environment of the excised disc space may present too great a challenge to the implant – it is well known that inflammation can lead to the breakdown of PG-rich structures. A strategy for transitioning engineered tissues from *in vitro* to *in vivo* may be required for successful tissue replacement. Likewise, resumption of mechanical loading may be required to maintain NP proteoglycan content. These are the focus of our current studies and will be the focus of future funding applications.

Key Research Accomplishments:

According to the progress we have made on the Aims outlined above, we have achieved the following Key Research Accomplishments.

- We have established advanced fabrication of DAPS AF regions, and have implemented new culture conditions to improve their maturation with time. (Aim 1)
- We have demonstrated that improvement of nutrient supply, via orbital shaking, improves the DAPS maturation process, suggesting that motion and flows encountered in vivo might improve maturation of constructs. (Aim 1)
- We have constructed and implemented a novel micro-torsion device and shown that DAPS improve in torsional properties with time in culture and shaking. (Aim 1)
- We have determined, with a focus on the NP region, that a short period of exposure to TGF at a high dose is equal to or better than long term exposure to this molecule. (Aim 1)
- We have shown that NP cells in HA perform well, and promote the NP cell phenotype. (Aim 1)
- We have fabricated full DAPS constructs based on native tissue cells (from the NP and AF) and MSCs, and coupled these with polymeric AF regions and hyaluronic acid (HA) based NP regions to form DAPS constructs. (Aim 1)
- We have evaluated the growth trajectory of the DAPS in vitro based on histological, molecular, biochemical, and mechanical outcomes. (Aim 1)
- We fully developed and validated a rat tail model of disc implantation (Aim 3), including the development of an external fixation system for protecting the implant during early stages of in vivo growth and maturation. (Aims 2&3)
- We successfully performed implantation of acellular engineered discs, and modified scaffolds to promote endogenous tissue infiltration. (Aims 2&3)
- We fabricated cell-based engineered discs of varying levels of maturity, and implanted these into the caudal spines of athymic rats and subcutaneously. (Aims 2&3)
- We developed MRI methods to evaluate the T2 signal within the NP and AF regions of the disc in the rat caudal spine. (Aim 3)
- We evaluated loss of T2 signal using our established MRI methods in our implanted engineered discs over a 1 week time course. (Aim 3)

Reportable Outcomes:

Based on funding from the DOD, our team has published three peer-reviewed manuscripts and have another 3 manuscripts that are either in review or about to be submitted based on this work. In addition, we published 15 abstracts at national and international meetings on this work. Funding from the DOD supported one doctoral student in mechanical engineering at the University of Pennsylvania as well as several postdoctoral fellows over the funding period.

Conclusions:

With support from the DOD, our team made marked progress over the last four years in the formation of DAPS into angle ply structures and optimization of the in vitro growth of both the AF and NP regions. We discovered important new methods to further this growth process, including a novel TGF dose and exposure regimens that generates a functional NP-like material. We also validated an in vivo rat tail model for the implantation of our DAPS construct, and designed novel fixation devices for protecting the DAPS post implantation. After successfully developing and validating our preclinical animal model, we evaluated both acellular and cellular implants. Cellular implants were based both on native tissue cells (from the AF or the NP) or mesenchymal stem cells. Data from these in vivo studies helped us to design better scaffolds with improved integration to the soft tissues in the disc space. Implantation of cell-based constructs, native cell and MSC-based, illustrated the differences between in vitro culture conditions and the complexity of the in vivo space. Specifically, we found that implant content and vitality in these cellularized, constructs was markedly affected by implantation, where we lost considerable PG from the NP region of the engineered disc. This observation changed, to some extent, the execution of Aim 3. We developed novel MR image processing tools to quantify disc structure and function, and then applied this methodology to our in vivo rat tail model to identify the time course over which the loss of PG content was occurring (especially in the NP). This analysis showed an almost complete loss of PG in the first week after implantation, suggesting that transition from in vitro to in vivo setting (including loss of pro-growth signals and inflammatory mediators in the implantation site) can compromise the integrity of the DAPS construct. We are now working on new methods to pre-condition the implant with 'in vivo-like' cues prior to implantation to harden it to the environment it will see with implantation (with funding received from the Department of Veterans' Affairs for a 4-year Merit Award). We are also exploring methods to delivery adjuvants that can improve synthesis and prevent degradation in the immediate time period around implantation so as to preserve engineered disc structure and function. We have also supported a new team member, Dr. Harvey Smith, in the acquisition of a new grant (a Career Development Award, with Dr. Mauck and Dr. Elliott as mentors) from the Department of Veterans' Affairs, with this work focused on translating the DAPS technology to the next stage of translation in a rabbit lumbar disc replacement model. Data derived from this funding have been critical in advancing the field of functional disc replacement, and have identified new challenges and opportunities that will be of great value in moving this work towards clinical realization.

References/Publications:

Full Length Manuscripts:

1. Martin JT, Milby AH, Chiaro JA, Kim DH, **Hebela** NM, Smith LJ, **Elliott** DM, **Mauck** RL (2014). Translation of an engineered nanofibrous disc-like angle ply structure for intervertebral disc replacement in a small animal model. *Acta Biomaterialia*; 10(6):2473-2481
2. Kim DH, Martin JT, **Elliott** DM, Smith LJ, **Mauck** RL (2015). Phenotypic stability, matrix elaboration and functional maturation of nucleus pulposus cells encapsulated in photocrosslinkable hyaluronic acid hydrogels. *Acta Biomater* 15(12):21-9.

3. Martin JT, Collins CM, Ikuta K, **Mauck** RL, **Elliott** DM, Zhang Y, Vaccaro AR, Albert TJ, Anderson DG, Collins CM, Smith HE (2015). Population average T2 MRI Maps reveal quantitative regional transformations in the degenerating rabbit intervertebral disc that vary by lumbar level. *J Orthop Res*; 33(1):140-148
4. Martin JT, Kim DH, Ikuta K, Pfeifer CG, Smith LJ, **Elliott** DM, Smith HE, **Mauck** RL (2015). In vitro growth trajectory and in vivo implantation of cell-seeded disc-like angle ply structures for total disc replacement. (in review)
5. Martin JT, Milby AH, Pfeifer CG, Smith LJ, **Elliott** DM Smith HE, **Mauck** RL (2015). Short and long-term outcomes with an acellular disc-like angle ply structure for total disc replacement in a small animal model. (in preparation)
6. Martin JT, Milby AH, Poudel S, Pfeifer CG, Smith HE, **Elliott** DM, **Mauck** RL (2015). A radiopaque electrospun scaffold for engineering fibrous tissues: characterization and *in vivo* application. (in review)

Abstracts and Conference Proceedings:

1. Kluge JA, Martin JT, Nerurkar NL, Amaniera FA, Pampati RA, **Elliott** DM, **Mauck** RL (2010). Functional enhancement of disc-like angle-ply structures via dynamic culture, *57th Annual Meeting of the Orthopaedic Research Society*, Long Beach, USA (Poster Presentation)
2. **Elliott** DM, Nerurkar NL, Huang AH, Kluge JA, Smith LJ, Martin JT, **Hebela** NM, **Mauck** RL (2010). Disc Tissue Engineering – Can We Make it Stick? *6th World Congress on Biomechanics*, Suntec City, Singapore (Keynote Presentation)
3. Martin JT, Smith LJ, Gorth DJ, **Hebela** NM, **Elliott** DM, **Mauck** RL (2012). Nanofibrous disc-like angle ply structures maintain rat caudal intervertebral disc height. *2012 Military Health System Research Symposium*, Fort Lauderdale, FL (Poster Presentation)
4. Kim DH, Smith LJ, Kim M, **Elliott** DM, **Mauck** RL (2013). Functional Maturation of a Cell-Seeded Hyaluronic Acid Hydrogel-Based Engineered Nucleus Pulposus. *Biomedical Engineering Society Annual Meeting*, Seattle, WA. (Poster Presentation)
5. Kim DH, Heo SJ, Smith LJ, **Elliott** DM, **Mauck** RL (2013). Different Response of Disc Cells to Variations in 3D and Mechanical Culture Conditions. *Biomedical Engineering Society Annual Meeting*, Seattle, WA. (Podium Presentation)
6. Martin JT, Smith LJ, Milby AH, Gorth DJ, Adan A, **Hebela** NM, **Elliott** DM, **Mauck** RL (2013). Nanofibrous disc-like angle ply structures maintain disc height in the rat caudal spine. *59th Annual Meeting of the Orthopaedic Research Society*, San Antonio, TX. (Poster Presentation)
7. Martin JT, Milby AH, Chiaro JA, **Hebela** NM, **Elliott** DM, **Mauck** RL (2013). Translation of a nanofibrous disc-like angle ply structure for intervertebral disc replacement in a small animal model. *Philadelphia Spine Research Society, Second International Spine Research Symposium*, Philadelphia, PA (Podium Presentation)
8. Martin JT, Milby AH, Chiaro JA, Kim DH, Smith LJ, Smith HE, **Elliott** DM, **Mauck** RL (2014). Engineered nanofibrous disc-like angle ply structures with sacrificial layers for

intervertebral disc replacement in a small animal model. *60th Annual Meeting of the Orthopaedic Research Society*, New Orleans, LA (Poster Presentation)

9. Martin JT, Poudel S, Milby AH, Pfeifer C, Smith HE, **Elliott** DM, **Mauck** RL (2014). A radiopaque electrospun scaffold for engineering fibrous tissues: characterization and in vivo application. 6*0th Annual Meeting of the Orthopaedic Research Society*, New Orleans, LA (Podium Presentation)
10. Kim DH, Smith LJ, **Elliott** DM, **Mauck** RL (2014). Maturation and Material Dependent Response of AF and NP Cells to Mechanical Perturbation. 6*0th Annual Meeting of the Orthopaedic Research Society*, New Orleans, LA (Poster Presentation)
11. Milby AH, Martin JT, Smith LJ, Chiaro JA, Smith HE, **Elliott** DM, **Mauck** RL (2014). Nanofibrous disc-like angle structures for intervertebral disc tissue engineering in a small animal model. *7th Annual Lumbar Spine Research Society Meeting*, Chicago, IL (Podium Presentation)
12. Martin JT, **Mauck** RL, Zhang Y, **Elliott** DM, Smith HE (2014). Population average T_2 MRI maps reveal quantitative transformations of the degenerating disc in a rabbit puncture model. *7th World Congress of Biomechanics*, Boston, MA (Poster Presentation)
13. Martin JT, Ikuta K, Kim DH, Pfeifer CG, Smith LJ, **Elliott** DM, Smith HE, **Mauck** RL (2015). *In vitro* growth trajectory and *in vivo* implantation of a cell-based disc-like angle ply structure for total disc replacement*. Philadelphia Spine Research Symposium* (Podium Presentation, Best Paper – Diagnostics and Therapeutics).
14. Martin JT, Collins CM, Ikuta K, **Mauck** RL, **Elliott** DM, Zhang Y, Anderson DG, Vaccaro AR, Albert TJ, Arlet V, Harvey HE (2015). Population average T2 MRI maps reveal quantitative regional transformations in the degenerating rabbit intervertebral disc that vary by lumbar level. *61st Annual Meeting of the Orthopaedic Research Society*, Las Vegas, NV (Poster Presentation)
15. Martin JT, Ikuta K, Kim DH, Pfeifer CG, Smith LJ, **Elliott** DM, Smith HE, **Mauck** RL (2015). *In vitro* growth trajectory and *in vivo* implantation of a cell-based disc-like angle ply structure for total disc replacement*. 61st Annual Meeting of the Orthopaedic Research Society*, Las Vegas, NV (Podium Presentation)

Appendices: N/A